

Hierarchical Optimal Transport for Unsupervised Domain Adaptation

Mourad El Hamri^{1,2,3}, Younès Bennani^{1,2}, Issam Falih^{2,4}, Hamid Ahaggach²

¹Laboratoire d'Informatique de Paris Nord, LIPN - CNRS UMR 7030, Université Sorbonne Paris Nord, France

²La Maison des Sciences Numériques - LaMSN, Université Sorbonne Paris Nord, France

³Dipartimento di Matematica, Università della Campania "Luigi Vanvitelli", Italy

⁴LIMOS - CNRS UMR 6518, Université Clermont Auvergne, France
name.surname@{sorbonne-paris-nord,uca}.fr

Abstract

In this paper, we propose a novel approach for unsupervised domain adaptation, that relates notions of optimal transport, learning probability measures and unsupervised learning. The proposed approach, HOT-DA, is based on a hierarchical formulation of optimal transport, that leverages beyond the geometrical information captured by the ground metric, richer structural information in the source and target domains. The additional information in the labeled source domain is formed instinctively by grouping samples into structures according to their class labels. While exploring hidden structures in the unlabeled target domain is reduced to the problem of learning probability measures through Wasserstein barycenter, which we prove to be equivalent to spectral clustering. Experiments on a toy dataset with controllable complexity and two challenging visual adaptation datasets show the superiority of the proposed approach over the state-of-the-art.

1 Introduction

Supervised learning is arguably the most widespread task of machine learning and has enjoyed much success on a broad spectrum of application domains (Kotsiantis et al. 2007). However, most supervised learning methods, are built on the crucial assumption that training and test data are drawn from the same probability distribution (Pan and Yang 2009). In real-world applications, this hypothesis is usually violated due to several application-dependent reasons: in computer vision, the presence or absence of backgrounds, the variation of acquisition devices or the change of lighting conditions introduce non-negligible discrepancies in data distributions (Saenko et al. 2010), in product reviews classification, the drift observed in the word distributions is caused by the difference of product category and the changes in word frequencies (Blitzer, Dredze, and Pereira 2007). These distributional shifts, will be likely to degrade significantly the generalization ability of supervised learning models. While manual labeling may appear as a feasible solution, such an approach is unreasonable in practice, since it is often prohibitively expensive to collect from scratch a new large high quality labeled dataset with the same distribution as the test data, due to lack of time, resources, or other factors, and it would be an immense waste to totally reject the available knowledge on a different,

yet related, labeled training set. Such a challenging situation has promoted the emergence of domain adaptation (Redko et al. 2019b), a sub-field of statistical learning theory (Vapnik 2013), that takes into account the distributional shift between training and test data, and in which the training set and test set distributions are respectively called source and target domains. There are two variants of domain adaptation problem, the unsupervised domain adaptation, where all the target data are unlabeled, and the semi-supervised domain adaptation, where few labeled target data are available. This paper deals with the challenging setting of unsupervised domain adaptation.

Since the launching of domain adaptation theory, a large panoply of algorithms were proposed to deal with its unsupervised variant, and they can be roughly divided into shallow (Kouw and Loog 2019) and deep (Wilson and Cook 2020) approaches. Most of shallow algorithms try to solve the unsupervised domain adaptation problem in two steps by first aligning the source and target domains to make them indiscernible, which then allows to apply traditional supervised methods on the transformed data. Such an alignment is typically accomplished through sample-based approaches which focus on correcting biases in the sampling procedure (Shimodaira 2000; Sugiyama et al. 2007) or feature-based approaches which focus on learning domain-invariant representations (Pan et al. 2010) and finding subspace mappings (Gong et al. 2012; Fernando et al. 2013). Deep domain adaptation algorithms have also gained a renewed interest due to their feature extraction ability to learn more abstract and robust representations that are both semantically meaningful and domain invariant. (Ganin et al. 2016) is one of the most popular deep adaptative networks, which is based on the adversarial training procedure (Goodfellow et al. 2014) and directly derived from the seminal theoretical contribution in (Ben-David et al. 2007), its main idea is to embed domain adaptation into the representation learning process, so that the final classification decisions are made based on features that are both discriminative and invariant to domain changes.

More recent advances in domain adaptation are due to the theory of optimal transport (Villani 2009), which allows to learn explicitly the least cost transformation of the source

distribution into the target one. This idea was first investigated in the work of (Courty et al. 2016) where authors have successfully casted the domain adaptation problem into an optimal transport problem between shifted marginal distributions of the two domains, which then allows to learn a classifier on the transported data. Since then, several optimal transport based domain adaptation methods have emerged. In (Courty et al. 2017), authors proposed to avoid the two-steps adaptation procedure, by aligning the joint distributions using a coupling accounting for the marginals and the class-conditional distributions shift jointly. Authors in (Redko et al. 2019a) performed multi-source domain adaptation under the target shift assumption by learning simultaneously the class probabilities of the unlabeled target samples and the optimal transport plan allowing to align several probability distributions. The recent work of (Dhouib, Redko, and Lartizien 2020) derived an efficient optimal transport based adversarial approach from a bound on the target margin violation rate, to name a few.

A common denominator of these approaches is their ability to capture the underlying geometry of the data by relying on the cost function that reflects the metric of the input space. However, these optimal transport based methods can benefit from not relying solely on such rudimentary geometrical information, since there is further important structural information that remains uncaptured directly from the ground metric, e.g., the local consistency structures induced by class labels in the source. The exploitation of these structures can induce some desired properties in domain adaptation like preserving compact classes during the transportation. It is, moreover, what led authors in (Courty et al. 2016) to propose the inclusion of these structural information by adding a group-norm regularizer. Such additional structures, however, could not be induced directly by the standard formulation of optimal transport. To the best of our knowledge, (Alvarez-Melis, Jaakkola, and Jegelka 2018) is the only work that has attempted to incorporate structural information directly into the optimal transport problem, without the need to add a regularized coefficient for expressing the class regularity constraints, by developing a nonlinear generalization of discrete optimal transport, based on submodular functions. However, the application of this method in domain adaptation only takes into account the available structures in the labeled source domain, by partitioning samples according to their class labels, while every target sample forms its own cluster. However, richer structures in the target domain can be easily captured differently, e.g., by grouping, and the incorporation of such target structures directly in the optimal transport formulation can lead in our view to a significant improvement in the performance of domain adaptation algorithms.

In this paper, we address the existing limitations of the target-structure-agnostic algorithms mentioned above by proposing a principally new approach based on hierarchical optimal transport (Schmitzer and Schnörr 2013). Hierarchical optimal transport, is an effective and efficient paradigm to induce structures in the transportation procedure. It has

been recently used for different tasks such as multi-level clustering (Ho et al. 2017), multimodal distribution alignment (Lee et al. 2019), document representation (Yurochkin et al. 2019) and semi-supervised learning (Taherkhani et al. 2020). The relevance of this paradigm for domain adaptation is illustrated in Figure 1, where we show that the structure-agnostic Reg-OT and target-structure-agnostic OT-GL algorithms fail to always restrict the transportation of mass across instances of different structures, whereas, our Hierarchical Optimal Transport for Domain Adaptation (HOT-DA) model manages to do it correctly by leveraging the source and target domain structures simultaneously.

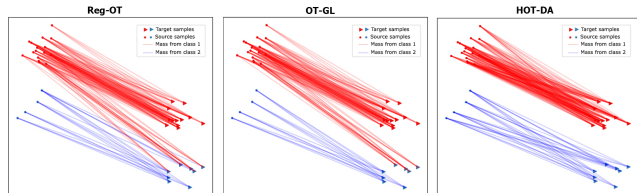


Figure 1: Illustration of the transportation obtained with structure-agnostic (Cuturi 2013) and target-structure-agnostic (Courty et al. 2016) methods, and with HOT-DA.

To the best of our knowledge, the proposed approach is the first hierarchical optimal transport method for unsupervised domain adaptation and the first work to shed light on the connection between spectral clustering and Wasserstein barycenter. The rest of this paper is organized as follows: in the 2nd section, we present a brief overview of unsupervised domain adaptation setup. In the 3rd section, we detail the optimal transport problem and its hierarchical formulation, then in the 4th section, we elaborate the HOT-DA method. Finally, in the last section, we evaluate our algorithm on a toy dataset and two benchmark visual adaptation problems.

2 Unsupervised domain adaptation

Let $\mathcal{X} = \mathbb{R}^d$ be an input space, $\mathcal{Y} = \{c_1, \dots, c_k\}$ a discrete label set consisting of k classes, \mathcal{S} and \mathcal{T} two different probability distributions over $\mathcal{X} \times \mathcal{Y}$ called respectively the source and target domains. We have access to a set $S = \{(x_i, y_i)\}_{i=1}^n$ of n labeled source samples drawn i.i.d. from the joint distribution \mathcal{S} and a set $T = \{x_j\}_{j=1}^m$ of m unlabeled target samples drawn i.i.d. from the marginal distribution $\mathcal{T}_{\mathcal{X}}$, of the joint distribution \mathcal{T} over \mathcal{X} , more formally:

$$S = \{(x_i, y_i)\}_{i=1}^n \sim (\mathcal{S})^n, \quad T = \{x_j\}_{j=1}^m \sim (\mathcal{T}_{\mathcal{X}})^m.$$

The aim of unsupervised domain adaptation algorithms is to infer a classifier $\eta : \mathcal{X} \rightarrow \mathcal{Y}$ with a low target risk:

$$\mathcal{R}_{\mathcal{T}}(\eta) = \mathbb{P}_{(x,y) \sim \mathcal{T}}(\eta(x) \neq y),$$

under the distributional shift assumption $\mathcal{S} \neq \mathcal{T}$, while having no information about the labels $\{y_j\}_{j=1}^m$ of the target set T . In the rest, we design by the source domain interchangeably the distribution \mathcal{S} and the labeled set S , and by the target domain, the distribution \mathcal{T} and the unlabeled set T .

3 Optimal Transport

In this section we present the key concepts of optimal transport problem and its hierarchical formulation (Villani 2009). Optimal transport is a long-standing mathematical problem whose theory has matured over the time. Its roots can be traced back to the 18th century, when the French mathematician Gaspard Monge introduced the following problem (Monge 1781): Let (\mathcal{X}, μ) and (\mathcal{Y}, ν) be two probability spaces, $c : \mathcal{X} \times \mathcal{Y} \rightarrow \mathbb{R}^+$ a positive cost function over $\mathcal{X} \times \mathcal{Y}$, which represents the work needed to move a mass unit from $x \in \mathcal{X}$ to $y \in \mathcal{Y}$. The problem asks to find a measurable transport map $\mathcal{T} : \mathcal{X} \rightarrow \mathcal{Y}$ that transports the mass represented by the probability measure μ to the mass represented by ν , while minimizing the total cost of this transportation,

$$(\mathcal{M}) \quad \inf_{\mathcal{T}} \left\{ \int_{\mathcal{X}} c(x, \mathcal{T}(x)) d\mu(x) \mid \mathcal{T}\#\mu = \nu \right\}, \quad (1)$$

where $\mathcal{T}\#\mu$ stands for the image measure of μ by \mathcal{T} . The problem of Monge (\mathcal{M}) is quit difficult, since it is not symmetric, and may not admit a solution, it is the case when μ is a Dirac measure and ν is not.

A long period of sleep followed Monge's formulation until the convex relaxation of the Soviet mathematician Leonid Kantorovitch in the thick of World War II (Kantorovich 1942). This relaxed formulation, known as the Monge-Kantorovich problem (\mathcal{MK}) allows mass splitting and, in contrast to the formulation of Monge, it guarantees the existence of a solution under very general assumptions,

$$(\mathcal{MK}) \quad \inf_{\gamma} \left\{ \int_{\mathcal{X} \times \mathcal{Y}} c(x, y) d\gamma(x, y) \mid \gamma \in \Pi(\mu, \nu) \right\}, \quad (2)$$

where $\Pi(\mu, \nu)$ is the transport plan set, constituted of joint probability measures γ on $\mathcal{X} \times \mathcal{Y}$ with marginals μ and ν , $\Pi(\mu, \nu) = \{\gamma \in \mathcal{P}(\mathcal{X} \times \mathcal{Y}) \mid \text{proj}_{\mathcal{X}}\#\gamma = \mu, \text{proj}_{\mathcal{Y}}\#\gamma = \nu\}$.

When $\mathcal{X} = \mathcal{Y}$ is a metric space endowed with a distance d , a natural choice is to use it as a cost function, e.g., $c(x, y) = d(x, y)^p$ for $p \in [1, +\infty[$. Then, the problem (\mathcal{MK}) induces a metric between probability measures over \mathcal{X} , called the p -Wasserstein distance (Santambrogio 2015), defined in the following way, $\forall \mu, \nu \in \mathcal{P}(\mathcal{X})$:

$$W_p(\mu, \nu) = \inf_{\gamma \in \Pi(\mu, \nu)} \left(\int_{\mathcal{X}^2} d^p(x, y) d\gamma(x, y) \right)^{1/p}, \quad (3)$$

In the discrete version of optimal transport, i.e., when the measures μ and ν are only available through discrete samples $X = (x_1, \dots, x_n) \subset \mathcal{X}$ and $Y = (y_1, \dots, y_m) \subset \mathcal{Y}$, their empirical distributions can be expressed as $\mu = \sum_{i=1}^n a_i \delta_{x_i}$ and $\nu = \sum_{j=1}^m b_j \delta_{y_j}$, where $a = (a_1, \dots, a_n)$ and $b = (b_1, \dots, b_m)$ are vectors in the probability simplex \sum_n and \sum_m respectively. The cost function only needs to be specified for every pair $(x_i, y_j)_{\substack{1 \leq i \leq n \\ 1 \leq j \leq m}} \in X \times Y$ yielding a

cost matrix $C \in \mathcal{M}_{n \times m}(\mathbb{R}^+)$. The optimal transport problem becomes then a linear program (Bertsimas and Tsitsiklis 1997), parametrized by the transportation polytope $U(a, b) = \{\gamma \in \mathcal{M}_{n \times m}(\mathbb{R}^+) \mid \gamma \mathbf{1}_m = a \text{ and } \gamma^T \mathbf{1}_n = b\}$,

which acts as a feasible set, and the matrix C which acts as a cost parameter. Thus, solving this linear program consists in finding a plan γ^* that realizes:

$$(\mathcal{D}_{\mathcal{MK}}) \quad \min_{\gamma \in U(a, b)} \langle \gamma, C \rangle_F, \quad (4)$$

where $\langle \cdot, \cdot \rangle_F$ is the Frobenius inner product. In this case, the p -Wasserstein distance is defined as: $W_p^p(\mu, \nu) = \langle \gamma^*, C \rangle_F$. Correlatively, a Wasserstein barycenter (Agueh and Carlier 2011) of N measures $\{\nu_1, \dots, \nu_N\}$ in $\mathcal{P}(\mathcal{X})$ can be defined as a minimizer of the following functional f over $\mathcal{P}(\mathcal{X})$:

$$f(\kappa) = \frac{1}{N} \sum_{i=1}^N \lambda_i W_p^p(\kappa, \nu_i), \quad (5)$$

where λ_i are positive real numbers such that $\sum_{i=1}^N \lambda_i = 1$.

As stated above, discrete optimal transport is a linear program, and thus can be solved exactly in $\mathcal{O}(r^3 \log(r))$, where $r = \max(n, m)$, with the simplex algorithm or interior point methods (Pele and Werman 2009), which is a heavy computational price tag. Entropy-regularization (Cuturi 2013) has emerged as a solution to the computational burden of optimal transport. The entropy-regularized discrete optimal transport problem is defined as follows:

$$(\mathcal{D}_{\mathcal{MK}}^\varepsilon) \quad \min_{\gamma \in U(a, b)} \langle \gamma, C \rangle_F - \varepsilon \mathcal{H}(\gamma), \quad (6)$$

where $\mathcal{H}(\gamma) = -\sum_{i=1}^n \sum_{j=1}^m \gamma_{ij} (\log(\gamma_{ij}) - 1)$ is the entropy of γ . This regularization allows a faster computation of the optimal transport plan (Peyré, Cuturi et al. 2019) in $\mathcal{O}(r^2/\varepsilon^3)$ (Altschuler, Weed, and Rigollet 2017) via the iterative procedure of Sinkhorn algorithm (Knight 2008).

Hierarchical optimal transport is an attractive formulation that offers an efficient way to induce structural information directly into the transportation process (Schmitzer and Schnörr 2013). Let \mathcal{X} be a Polish metric space endowed with a distance d and $\mathcal{P}(\mathcal{X})$ be the space of Borel probability measures on \mathcal{X} equipped with the Wasserstein distance W_p according to (3). Since \mathcal{X} is a Polish metric space, then $\mathcal{P}(\mathcal{X})$ is also a Polish metric space (Parthasarathy 2005). By a recursion of concepts, $\mathcal{P}(\mathcal{P}(\mathcal{X}))$ the space of Borel probability measures on $\mathcal{P}(\mathcal{X})$ is a Polish metric space, and will be equipped also with a Wasserstein metric W_p' induced this time by the Wasserstein distance W_p which acts as the ground metric on $\mathcal{P}(\mathcal{X})$. More formally, let $\theta = (\mu_1, \dots, \mu_h)$ and $\vartheta = (\nu_1, \dots, \nu_l)$ be two set of probability measures over $\mathcal{P}(\mathcal{X})$, i.e., $\theta, \vartheta \subset \mathcal{P}(\mathcal{X})$. The empirical distributions of θ and ϑ can be expressed respectively by $\phi, \varphi \in \mathcal{P}(\mathcal{P}(\mathcal{X}))$ as $\phi = \sum_{i=1}^h \alpha_i \delta_{\mu_i}$ and $\varphi = \sum_{j=1}^l \beta_j \delta_{\nu_j}$, where $\alpha = (\alpha_1, \dots, \alpha_h)$ and $\beta = (\beta_1, \dots, \beta_l)$ are vectors in the probability simplex \sum_h and \sum_l respectively. Then, the hierarchical optimal transport problem between ϕ and φ is:

$$(\mathcal{HOT}) \quad \min_{\Gamma \in U(\alpha, \beta)} \langle \Gamma, \mathcal{W} \rangle_F, \quad (7)$$

where the matrix $\mathcal{W} = (W_p(\mu_i, \nu_j))_{\substack{1 \leq i \leq h \\ 1 \leq j \leq l}} \in \mathcal{M}_{h \times l}(\mathbb{R}^+)$,

stands for the new cost parameter and $U(\alpha, \beta)$ represents the new transportation polytope defined in the following way: $U(\alpha, \beta) = \{\Gamma \in \mathcal{M}_{h \times l}(\mathbb{R}^+) \mid \Gamma \mathbf{1}_l = \alpha \text{ and } \Gamma^T \mathbf{1}_h = \beta\}$.

4 HOT-DA: Hierarchical Optimal Transport for Unsupervised Domain Adaptation

In this section, we introduce the proposed HOT-DA approach, that consists of three phases, the first one aims to learn hidden structures in the unlabeled target domain using Wasserstein barycenter, which we prove can be equivalent to spectral clustering, the second phase focuses on finding a one-to-one matching between structures of the two domains through the hierarchical optimal transport formulation, and the third phase involves transporting samples of each source structure to its corresponding target structure via the barycentric mapping.

4.1 Learning unlabeled target structures through Wasserstein-Spectral clustering

Samples in the source domain $S = \{(x_i, y_i)\}_{i=1}^n$ can be grouped into structures according to their class labels, but, data in the target domain $T = \{x_j\}_{j=1}^m$ are not labeled to allow us to identify directly such structures. Removing this obstacle cannot be accomplished without using some additional assumptions. In fact, to exploit efficiently the unlabeled data in the target domain, the most plausible assumption stems from the structural hypothesis based on clustering, where it is assumed that the data belonging to the same cluster are more likely to share the same label. This assumption constitutes the core nucleus for the first phase of our approach, which aims to prove that spectral clustering can be casted as a problem of learning probability measures with respect to Wasserstein barycenter. Our proof is based on three key ingredients: the equivalence between the search for a 2-Wasserstein barycenter of the empirical distribution that represents unlabeled data and k -means clustering, the analogy between traditional k -means and kernel k -means and finally the connection between kernel k -means and spectral clustering. We derive from this result a novel algorithm able to learn efficiently hidden structures of arbitrary shapes in the unlabeled target domain.

Firstly, given m unlabeled instances $\{x_1, \dots, x_m\} \subset \mathcal{X}$, k -means clustering (MacQueen et al. 1967) aims to partition the m samples into k clusters $\Pi_k = \{\pi_1, \dots, \pi_k\}$ in which each sample belongs to the cluster with the nearest center. This results in a partitioning of the data space into Voronoi cells $(\text{Vor}_q)_{1 \leq q \leq k}$ generated by the cluster centers $\tilde{C}_k = \{c_1, \dots, c_k\}$. The goal of k -means then is to minimize the mean squared error, and its objective is defined as:

$$\min_{c_1, \dots, c_k} \frac{1}{m} \sum_{i=1}^m \|x_i - c_j\|^2, \quad (8)$$

Let $\hat{\rho}_m = \sum_{i=1}^m \frac{1}{m} \delta_{x_i}$ be the empirical distribution of $\{x_1, \dots, x_m\}$. Since $\frac{1}{m} \sum_{i=1}^m \|x_i - c_j\|^2 = \mathbb{E}_{x \sim \hat{\rho}_m} \|x - \tilde{C}_k\|^2$, then according to (Canas and Rosasco 2012):

$$\frac{1}{m} \sum_{i=1}^m \|x_i - c_j\|^2 = W_2^2(\hat{\rho}_m, \pi_{\tilde{C}_k} \# \hat{\rho}_m), \quad (9)$$

where $\pi_{\tilde{C}_k} : \mathcal{X} \rightarrow \tilde{C}_k$ is the projection function mapping each $x \in \text{Vor}_q \subset \mathcal{X}$ to c_q . Since k -means minimizes (9), it

also finds the measure that is closest to $\hat{\rho}_m$ among those with support of size k (Pollard 1982). Which proves the equivalence between k -means and searching for a 2-Wasserstein barycenter of $\hat{\rho}_m$ in $\mathcal{P}_k(\mathcal{X})$, i.e., a minimizer in $\mathcal{P}_k(\mathcal{X})$ of:

$$f(\kappa) = W_2^2(\hat{\rho}_m, \kappa), \quad (10)$$

Secondly, k -means suffers from a major drawback, namely that it cannot separate clusters that are nonlinearly separable in the input space. Kernel k -means (Schölkopf, Smola, and Müller 1998) can overcome this limitation by mapping the input data in \mathcal{X} to a high-dimensional reproducing kernel Hilbert space \mathcal{H} by a nonlinear mapping $\psi : \mathcal{X} \rightarrow \mathcal{H}$, then the traditional k -means is applied on the high-dimensional mappings $\{\psi(x_1), \dots, \psi(x_m)\}$ to obtain a nonlinear partition. Thus, the objective function of kernel k -means can be expressed analogously to that of traditional k -means in (8):

$$\min_{c_1, \dots, c_k} \frac{1}{m} \sum_{i=1}^m \|\psi(x_i) - c_j\|^2, \quad (11)$$

Usually the nonlinear mapping $\psi(x_i)$ cannot be explicitly computed, instead, the inner product of any two mappings $\psi(x_i)^T \psi(x_j)$ can be computed by a kernel function \mathcal{K} . Hence, the whole data set in the high-dimensional space can be represented by a kernel matrix $K \in \mathcal{M}_m(\mathbb{R}^+)$, where each entry is defined as: $K_{i,j} = \mathcal{K}(x_i, x_j) = \psi(x_i)^T \psi(x_j)$.

Thirdly, according to (Zha et al. 2001), the objective function of kernel k -means in (11) can be transformed to the following spectral relaxed maximization problem:

$$\max_{Y^T Y = I_k, Y \geq 0} \text{trace}(Y^T K Y), \quad (12)$$

On the other hand, spectral clustering has emerged as a robust approach for data clustering (Shi and Malik 2000; Ng, Jordan, and Weiss 2002). Here we focus on the normalized cut for k -way clustering objective function (Gu et al. 2001; Stella and Shi 2003). Let $G = (V, E, \tilde{K})$ be a weighted graph, where $V = \{x_1, \dots, x_m\}$ is the vertex set, E the edge set, and \tilde{K} the affinity matrix defined by a kernel \tilde{K} . The k -way normalized cut spectral clustering aims to find a disjoint partition $\{V_1, \dots, V_k\}$ of the vertex set V , such that:

$$\min_{V_1, \dots, V_k} \sum_{l=1}^k \text{linkratio}(V_l, \bar{V}_l), \quad (13)$$

where $\text{linkratio}(V_l, \bar{V}_l) = \frac{\text{links}(V_l, \bar{V}_l)}{\text{degree}(V_l)} = \frac{\sum_{i \in V_l} \sum_{j \in \bar{V}_l} \tilde{K}_{ij}}{\sum_{i \in V_l} \sum_{j \in V} \tilde{K}_{ij}}$.

Following (Dhillon, Guan, and Kulis 2004; Ding, He, and Simon 2005), the minimization in (13) can be casted as:

$$\max_{Z^T Z = I_k, Z \geq 0} \text{trace}(Z^T \tilde{D}^{-1/2} \tilde{K} \tilde{D}^{-1/2} Z), \quad (14)$$

where \tilde{D} is the degree matrix of the graph G . Thus, the maximization problem in (14) is identical to the spectral relaxed maximization of kernel k -means clustering in (12) when equipped with the kernel matrix $K = \tilde{D}^{-1/2} \tilde{K} \tilde{D}^{-1/2}$.

According to the three-dimensional analysis above, we can now give the main result in the 1st phase of our method:

Theorem 1 *Spectral clustering using an affinity matrix \tilde{K} is equivalent to the search for a 2-Wasserstein barycenter of $\hat{\varrho}_m = \sum_{i=1}^m \frac{1}{m} \delta_{\xi(x_i)}$ in the space of probability measures with support of size k , where ξ is a nonlinear mapping corresponding to the kernel matrix $K = \tilde{D}^{-1/2} \tilde{K} \tilde{D}^{-1/2}$.*

In the sequel, we will refer to the search for a 2-Wasserstein barycenter of $\hat{\varrho}_m$ as Wasserstein-Spectral clustering, and we will use it to learn k hidden structures in the unlabeled target domain T . There are fast and efficient algorithms to perform Wasserstein-Spectral clustering (Cuturi and Doucet 2014), which offers an alternative to the popular spectral clustering algorithm of (Ng, Jordan, and Weiss 2002).

The theoretical result in Theorem 1 is confirmed by experiments, this is illustrated in Figure 2, where we show that Wasserstein-Spectral clustering performs identically to the traditional spectral clustering, and that both are effective at separating clusters that are nonlinearly separable, whereas k -means fails to separate data with non-globular structures.

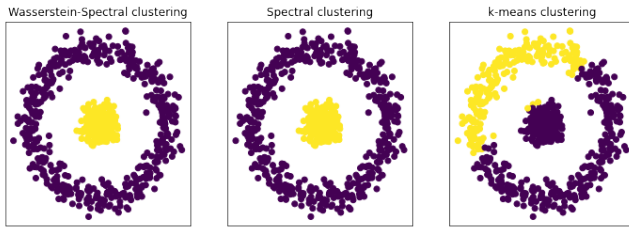


Figure 2: Comparison of Wasserstein-Spectral clustering, spectral clustering and k -means on Two-Circles dataset.

4.2 Matching source and target structures through hierarchical optimal transport

Optimal transport offers a well-founded geometric way for comparing probability measures in a Lagrangian framework, and for inferring a matching between them as an inherent part of its computation. Its hierarchical formulation has inherited all these properties with the extra benefit of inducing structural information directly without the need to add any regularized term for this purpose, as well as the capability to split a sophisticated optimization surface into simpler ones that are less subject to local minima, and the ability to benefit from the entropy-regularization. Hence the key insight behind its use in the second phase of our method.

To use an appropriate formulation for hierarchical optimal transport, samples in the source domain $S = \{(x_i, y_i)\}_{i=1}^n$ must be partitioning according to their class labels $y_i \in \mathcal{Y} = \{c_1, \dots, c_k\}$ into k classes $\{C_1, \dots, C_k\}$. The empirical distributions of these structures can be expressed using discrete measures $\{\mu_1, \dots, \mu_k\} \subset \mathcal{P}(\mathcal{X})$ as follows:

$$\mu_h = \sum_{i=1/x_i \in C_h}^n a_i \delta_{x_i}, \quad \forall h \in \{1, \dots, k\} \quad (15)$$

Similarly, samples in the target domain $T = \{x_j\}_{j=1}^m$ are grouped in k clusters $\{Cl_1, \dots, Cl_k\}$ using Wasserstein-

Spectral clustering in the first phase. The empirical distributions of these structures can be expressed using discrete measures $\{\nu_1, \dots, \nu_k\} \subset \mathcal{P}(\mathcal{X})$ in the following way:

$$\nu_l = \sum_{j=1/x_j \in Cl_l}^m b_j \delta_{x_j}, \quad \forall l \in \{1, \dots, k\} \quad (16)$$

Under the assumption that S and T are two collections of independent and identically distributed samples, the weights of all instances in each structure are naturally set to be equal:

$$\alpha_i = \frac{1}{|C_h|} \quad \text{and} \quad b_j = \frac{1}{|Cl_l|}, \quad \forall h, l \in \{1, \dots, k\}$$

All the labeled data in the source domain S and the unlabeled data in the target domain T can be seen in a hierarchical paradigm as a collection of classes and clusters. Thus, the distribution of S and T can be expressed respectively as a measure of measures ϕ and φ in $\mathcal{P}(\mathcal{P}(\mathcal{X}))$ as follows:

$$\phi = \sum_{h=1}^k \alpha_h \delta_{\mu_h} \quad \text{and} \quad \varphi = \sum_{l=1}^k \beta_l \delta_{\nu_l}, \quad (17)$$

where $\alpha = (\alpha_1, \dots, \alpha_k)$ and $\beta = (\beta_1, \dots, \beta_k)$ are vectors in the probability simplex \sum_k . The weights α_h and β_l reflect the cardinality of the class C_h in S and the cluster Cl_l in T :

$$\alpha_h = \frac{|C_h|}{n} \quad \text{and} \quad \beta_l = \frac{|Cl_l|}{m}, \quad \forall h, l \in \{1, \dots, k\}$$

To learn the correspondence between classes and clusters, we formulate an entropy-regularized hierarchical optimal transport problem between ϕ and φ in the following way:

$$(\mathcal{HOT}\text{-DA}) \quad \min_{\Gamma \in U(\alpha, \beta)} \langle \Gamma, \mathcal{W} \rangle_F - \varepsilon \mathcal{H}(\Gamma), \quad (18)$$

where $U(\alpha, \beta)$ represents the transportation polytope: $U(\alpha, \beta) = \{\Gamma \in \mathcal{M}_k(\mathbb{R}^+) \mid \Gamma \mathbf{1}_k = \alpha \text{ and } \Gamma^T \mathbf{1}_k = \beta\}$. $\mathcal{W} = (\mathcal{W}_{h,l})_{1 \leq h, l \leq k} \in \mathcal{M}_k(\mathbb{R}^+)$ stands for the cost matrix, whose each matrix-entry $\mathcal{W}_{h,l}$ is defined as the p -Wasserstein distance between the measures μ_h and ν_l , with:

$$\mathcal{W}_{h,l}^p = W_p^p(\mu_h, \nu_l) = \langle \gamma_{h,l}^{*, \varepsilon'}, \mathcal{C}_{h,l} \rangle_F, \quad (19)$$

where $\mathcal{C}_{h,l}$ is the cost matrix of pairwise squared-Euclidean distances between elements of C_h and Cl_l , and $\gamma_{h,l}^{*, \varepsilon'}$ is the regularized optimal transport plan between μ_h and ν_l .

The optimal transport plan Γ_ε^* of (18) can be interpreted as a soft multivalued matching between ϕ and φ as it provides the degree of association between classes $\{C_1, \dots, C_k\}$ in the source domain S and clusters $\{Cl_1, \dots, Cl_k\}$ in the target domain T . Then, the symmetric one-to-one matching relationship ($\hat{=}$) between each class C_h and its corresponding cluster Cl_l can be inferred by hard assignment from Γ_ε^* :

$$C_h \hat{=} Cl_l \mid l = \underset{j=1, \dots, k}{\operatorname{argmax}} \Gamma_\varepsilon^*(h, j), \quad \forall h \in \{1, \dots, k\} \quad (20)$$

4.3 Transporting source to target structures through the barycentric mapping

Besides being a means of comparison and matching, optimal transport has the asset of performing, as an intrinsic property of its transportation quiddity, an alignment of probability measures. Hence the main underlying idea of this phase.

Once the correspondence between source and target structures has been determined according to the one-to-one matching relationship ($\hat{\equiv}$) in (20), the source samples in each class C_h have to be transported to the target samples in the corresponding cluster Cl_l . This transportation can be handily expressed for each instance x_i in C_h with respect to the instances in Cl_l as the following barycentric mapping (Reich 2013; Ferradans et al. 2014; Courty et al. 2016):

$$\tilde{x}_i = \underset{x \in \mathcal{X}}{\operatorname{argmin}} \sum_{j=1/x_j \in Cl_l}^m \gamma_{h,l}^{*,\varepsilon'}(i,j) \|x - x_j\|^2 \quad (21)$$

where \tilde{x}_i is the image of x_i in the region occupied by Cl_l on the target domain, and $\gamma_{h,l}^{*,\varepsilon'}$ is the optimal transport plan between μ_h and ν_l already computed in (19). The barycentric mapping can be formulated for each class C_h as follows:

$$\tilde{C}_h = \operatorname{diag}(\gamma_{h,l}^{*,\varepsilon'} \mathbf{1}_{|Cl_l|})^{-1} \gamma_{h,l}^{*,\varepsilon'} Cl_l \quad \forall h \in \{1, \dots, k\} \quad (22)$$

While samples in C_h and Cl_l are drawn i.i.d. from μ_h and ν_l , then this mapping can be casted as a linear expression:

$$\tilde{C}_h = |C_h| \gamma_{h,l}^{*,\varepsilon'} Cl_l \quad \forall h \in \{1, \dots, k\} \quad (23)$$

After the alignment of each class C_h with its corresponding cluster Cl_l has been done as suggested in (23), a classifier η can be learned on the transported labeled data $\tilde{S} = \cup_{q=1}^k \tilde{C}_q$ and evaluated on the unlabeled target data T . The proposed HOT-DA approach is formally summarized in Algorithm 1:

Algorithm 1: HOT-DA

Input : $S = \{(x_i, y_i)\}_{i=1}^n, T = \{x_j\}_{j=1}^m$

Parameter: $\varepsilon, \varepsilon'$

- 1: Form $\mu_h, \nu_l \quad \forall h, l \in \{1, \dots, k\}$ (15,16)
 - 2: Form ϕ, φ (17)
 - 3: Solve the HOT-DA problem between ϕ and φ (18)
 - 4: Get the one-to-one matching between structures (20)
 - 5: Transport the source structures to the target ones (23)
 - 6: Train a classifier η on \tilde{S} and evaluate it on T
 - 7: **return** $\{y_j\}_{j=1}^m$
-

5 Experimental Results

In this section, we evaluate our method on a toy dataset and two challenging real world visual adaptation tasks¹.

5.1 Inter-twinning moons dataset

In the first experiment, we carry on moons dataset, the source domain is the classical binary two inter-twinning moons centered at the origin (0,0) and composed of 300 instances, where each class is associated to one moon of 150 samples. We consider 7 different target domains by rotating anticlockwise the source domain around its center according to 7 angles. Naturally, the greater is the angle, the

¹We make our code and the used datasets publicly available at: <https://github.com/HOT-DA/HOT-DA>

harder is the adaptation. The experiments were run by setting $\varepsilon = \varepsilon' = 0.1$, and an SVM with a Gaussian kernel as classifier, whose width parameter was chosen as $\sigma = \frac{1}{2\sqrt{V}}$, where V is the variance of the transported source samples. Our algorithm is compared to an SVM classifier with a Gaussian kernel trained on the source domain (without adaptation) and three optimal transport based domain adaptation methods, OT-GL (Courty et al. 2016), JDOT (Courty et al. 2017) and MADAOT (Dhouib, Redko, and Lartizien 2020), with the hyperparameter ranges suggested by their authors. To assess the generalization ability of the compared methods, they are tested on an independent set of 1000 instances that follow the same distribution as the target domain. The experiments are conducted 10 times, and the average accuracy is considered as a comparison criterion. The results are presented in Table 1.

Angle (°)	10°	20°	30°	40°	50°	70°	90°
SVM	1	0.896	0.760	0.688	0.600	0.266	0.172
OT-GL	1	1	1	0.987	0.804	0.622	0.492
JDOT	0.989	0.955	0.906	0.865	0.815	0.705	0.600
MADAOT	0.995	0.993	0.996	0.996	0.989	0.770	0.641
HOT-DA	1	1	1	1	1	0.999	0.970

Table 1: Average accuracy over 10 realizations in moons dataset for 7 rotation angles

We remark that all the considered algorithms based on optimal transport manage to achieve an almost perfect score on the angles from 10° to 40°, which is rational, as for these small angles the adaptation problem remains quite easy. However, the SVM without adaptation has experienced a decline of almost one third of its accuracy from 30°. Which proves that moons dataset presents a difficult adaptation problem that goes beyond the generalization ability of standard supervised learning models. For the strongest deformation, from 50° and up to 90°, our method always provides an almost perfect score, while a considerable deterioration in the performance of OT-GL and JDOT from 50° and also of MADAOT from 70° was observed. In short, structures leveraged by HOT-DA are highlighted by eliminating the increasing difficulty of this adaptation task, the constancy of the excellent performances of our approach speaks for itself.

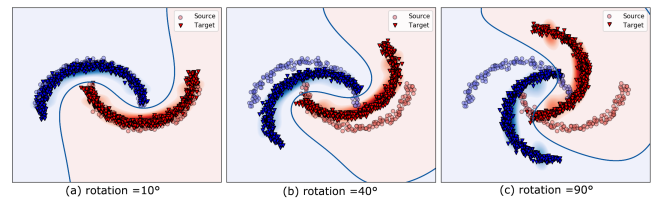


Figure 3: Illustration of the decision boundary of HOT-DA over moons problem for increasing rotation angles.

5.2 Visual adaptation datasets

We now evaluate our method on two challenging problems. We start by presenting the datasets, the experimental setting,

and finish by providing and discussing the obtained results.

Datasets: We consider two visual adaptation problems. A detailed description of each problem is given in Table 2.

Problem	Domains	Dataset	#Samples	#Features	#Classes	Abbr.
Digits	USPS	USPS	1800	256	10	U
	MNIST	MNIST	2000	256	10	M
Objects	Caltech	Caltech	1123	4096	10	C
	Amazon	Office	958	4096	10	A
	Webcam	Office	295	4096	10	W
	DSLR	Office	157	4096	10	D

Table 2: Description of the visual adaptation problems

Experimental protocol and hyper-parameter tuning:

For the first problem of digits recognition, 2000 and 1800 images are randomly selected respectively from the original MNIST and USPS datasets. Then, the selected MNIST images are resized to the same 16×16 resolution as USPS ones. For the second problem of objects recognition, Caltech-Office dataset is used, where we randomly sampled a collection of 20 instances per class from each domain, except for DSLR where only 8 instances per class are selected. For this problem, 4096 DeCaf6 features are used to represent the images (Donahue et al. 2014). As a classifier for our approach we use 1-Nearest Neighbor classifier (1NN). The comparison is then conducted using 1NN classifier (without adaptation) and four domain adaptation methods, SA (Fernando et al. 2013) with a linear SVM, JDA (Long et al. 2013) with 1NN classifier, OT-GL with 1NN classifier (Courty et al. 2016) and JDOT with a linear SVM (Courty et al. 2017). For digits recognition problem, the experiment was run by setting $\varepsilon = \varepsilon' = 0.5$. As for objects recognition problem, each target domain is equitably split on a validation and test sets. The validation set is used to select the best hyper-parameters $\varepsilon, \varepsilon'$ in the range of $\{1, \dots, 100\}$. The accuracy, is then evaluated on the test set, with the chosen hyper-parameter values. The experimentation is performed 10 times, and the mean accuracy in % is reported.

Results: The results of our experiments are reported in Table 3. From this table, we see that HOT-DA outperforms the other methods on 9 out of 14 tasks, and has the second best accuracy on another task. The table also present the average results of each algorithm, which confirm the superiority of our approach over the other methods in the two problems. Therefore, we attribute this performance gain to the effectiveness of our Wasserstein-Spectral clustering that succeeds in learning hidden structures in the target domain even if they do not have compact and globular shapes, which is the case in these two challenging visual adaptation problems. Furthermore, the hierarchical formulation efficiently incorporates these structures, which allows to preserve compact classes during the transportation and limits the mass splitting across different target structures.

Task	1NN	JDA	SA	OT-GL	JDOT	HOT-DA
M \rightarrow U	58.33	60.09	67.71	69.96	64.00	74.94
U \rightarrow M	39.00	54.52	49.85	57.85	56.00	63.30
average	48.66	57.30	58.73	63.90	60.00	69.12
A \rightarrow C	22.25	81.28	79.20	85.51	85.22	83.33
A \rightarrow D	20.38	86.25	83.80	85.00	87.90	93.33
A \rightarrow W	23.51	88.33	74.60	83.05	84.75	95.10
C \rightarrow A	20.54	88.04	89.30	92.08	91.54	92.14
C \rightarrow D	19.62	84.12	74.40	87.25	89.91	90.65
C \rightarrow W	18.94	79.60	88.50	84.17	88.81	94.69
D \rightarrow A	27.10	91.32	79.00	92.31	88.10	91.33
D \rightarrow C	23.97	81.13	92.25	84.11	84.33	78.28
D \rightarrow W	51.26	97.48	79.20	96.29	96.61	97.50
W \rightarrow A	23.19	90.19	55.00	90.62	90.71	90.92
W \rightarrow C	19.29	81.97	99.60	81.45	82.64	72.04
W \rightarrow D	53.62	98.88	81.65	96.25	98.09	95.32
average	28.47	86.72	81.65	88.18	89.05	89.54

Table 3: Accuracy over the two visual adaptation datasets

6 Conclusion

In this paper we proposed HOT-DA, a novel approach dealing with unsupervised domain adaptation, by leveraging the ability of hierarchical optimal transport to induce structural information directly into the transportation process. We also proved the equivalence between spectral clustering and the problem of learning probability measures through Wasserstein barycenter, this latter was used to learn hidden structures in the unlabeled target domain as a seminal step before performing hierarchical optimal transport. The algorithm derived from the established approach, has proved to be efficient on both simulated and real-world problems compared to several state-of-the-art methods. In the future, we plan to improve the efficiency of HOT-DA by a deep learning extension to handle larger and more complex datasets.

References

- Agueh, M.; and Carlier, G. 2011. Barycenters in the Wasserstein space. *SIAM Journal on Mathematical Analysis*, 43(2): 904–924.
- Altschuler, J.; Weed, J.; and Rigollet, P. 2017. Near-Linear Time Approximation Algorithms for Optimal Transport via Sinkhorn Iteration. *NIPS'17*, 1961–1971.
- Alvarez-Melis, D.; Jaakkola, T.; and Jegelka, S. 2018. Structured optimal transport. In *International Conference on Artificial Intelligence and Statistics*, 1771–1780. PMLR.
- Ben-David, S.; Blitzer, J.; Crammer, K.; Pereira, F.; et al. 2007. Analysis of representations for domain adaptation. *Advances in neural information processing systems*, 19: 137.
- Bertsimas, D.; and Tsitsiklis, J. N. 1997. *Introduction to linear optimization*, volume 6. Athena Scientific Belmont, MA.
- Blitzer, J.; Dredze, M.; and Pereira, F. 2007. Biographies, bollywood, boom-boxes and blenders: Domain adaptation for sentiment classification. In *45th annual meeting of the ACL*.
- Canas, G.; and Rosasco, L. 2012. Learning Probability Measures with respect to Optimal Transport Metrics. In *Advances in Neural Information Processing Systems*, volume 25.
- Courty, N.; Flamary, R.; Habrard, A.; and Rakotomamonjy, A. 2017. Joint distribution optimal transportation for domain adaptation. In *Advances in Neural Information Processing Systems*.

- Courty, N.; Flamary, R.; Tuia, D.; and Rakotomamonjy, A. 2016. Optimal transport for domain adaptation. *IEEE transactions on pattern analysis and machine intelligence*, 39(9): 1853–1865.
- Cuturi, M. 2013. Sinkhorn distances: Lightspeed computation of optimal transport. *Advances in neural information processing systems*, 26: 2292–2300.
- Cuturi, M.; and Doucet, A. 2014. Fast computation of Wasserstein barycenters. In *International conference on machine learning*, 685–693. PMLR.
- Dhillon, I.; Guan, Y.; and Kulis, B. 2004. Kernel k-means: spectral clustering and normalized cuts. In *Proceedings of the tenth international conference on Knowledge discovery and data mining*.
- Dhouib, S.; Redko, I.; and Lartizien, C. 2020. Margin-aware adversarial domain adaptation with optimal transport. In *International Conference on Machine Learning*, 2514–2524. PMLR.
- Ding, C.; He, X.; and Simon, H. D. 2005. On the equivalence of nonnegative matrix factorization and spectral clustering. In *Proceedings of the SIAM international conference on data mining*.
- Donahue, J.; Jia, Y.; Vinyals, O.; Hoffman, J.; Zhang, N.; Tzeng, E.; and Darrell, T. 2014. Decaf: A deep convolutional activation feature for generic visual recognition. In *ICML*, 647–655. PMLR.
- Fernando, B.; Habrard, A.; Sebban, M.; and Tuytelaars, T. 2013. Unsupervised visual domain adaptation using subspace alignment. In *Proceedings of the IEEE ICCV*, 2960–2967.
- Ferradans, S.; Papadakis, N.; Peyré, G.; and Aujol, J.-F. 2014. Regularized discrete optimal transport. *SIAM Journal on Imaging Sciences*, 7(3): 1853–1882.
- Ganin, Y.; Ustinova, E.; Ajakan, H.; Germain, P.; Larochelle, H.; Laviolette, F.; Marchand, M.; and Lempitsky, V. 2016. Domain-adversarial training of neural networks. *JMLR*, 17(1): 2096–2030.
- Gong, B.; Shi, Y.; Sha, F.; and Grauman, K. 2012. Geodesic flow kernel for unsupervised domain adaptation. In *2012 IEEE conference on computer vision and pattern recognition*, 2066–2073.
- Goodfellow, I.; Pouget-Abadie, J.; Mirza, M.; Xu, B.; Warde-Farley, D.; Ozair, S.; Courville, A.; and Bengio, Y. 2014. Generative adversarial nets. *NIPS'14*.
- Gu, M.; Zha, H.; Ding, C.; He, X.; Simon, H.; and Xia, J. 2001. Spectral relaxation models and structure analysis for k-way graph clustering and bi-clustering.
- Ho, N.; Nguyen, X.; Yurochkin, M.; Bui, H. H.; Huynh, V.; and Phung, D. 2017. Multilevel clustering via Wasserstein means. In *International Conference on Machine Learning*, 1501–1509.
- Kantorovich, L. V. 1942. On the translocation of masses. In *Dokl. Akad. Nauk. USSR (NS)*, volume 37, 199–201.
- Knight, P. A. 2008. The Sinkhorn–Knopp algorithm: convergence and applications. *SIAM Journal on Matrix Analysis and Applications*, 30(1): 261–275.
- Kotsiantis, S. B.; Zaharakis, I.; Pintelas, P.; et al. 2007. Supervised machine learning: A review of classification techniques. *Emerging artificial intelligence applications in computer engineering*, 3–24.
- Kouw, W. M.; and Loog, M. 2019. A review of domain adaptation without target labels. *IEEE transactions on pattern analysis and machine intelligence*, 43(3): 766–785.
- Lee, J.; Dabagia, M.; Dyer, E.; and Rozell, C. 2019. Hierarchical Optimal Transport for Multimodal Distribution Alignment. In *Advances in Neural Information Processing Systems*, volume 32.
- Long, M.; Wang, J.; Ding, G.; Sun, J.; and Yu, P. S. 2013. Transfer feature learning with joint distribution adaptation. In *Proceedings of the IEEE international conference on computer vision*.
- MacQueen, J.; et al. 1967. Some methods for classification and analysis of multivariate observations. In *Proceedings of the fifth Berkeley symposium on mathematical statistics and probability*.
- Monge, G. 1781. Mémoire sur la théorie des déblais et des remblais. *Histoire de l'Académie Royale des Sciences de Paris*.
- Ng, A. Y.; Jordan, M. I.; and Weiss, Y. 2002. On spectral clustering: Analysis and an algorithm. In *Advances in neural information processing systems*, 849–856.
- Pan, S. J.; Tsang, I. W.; Kwok, J. T.; and Yang, Q. 2010. Domain adaptation via transfer component analysis. *IEEE transactions on neural networks*, 22(2): 199–210.
- Pan, S. J.; and Yang, Q. 2009. A survey on transfer learning. *IEEE Transactions on knowledge and data engineering*, 22(10).
- Parthasarathy, K. R. 2005. *Probability measures on metric spaces*, volume 352. American Mathematical Soc.
- Pele, O.; and Werman, M. 2009. Fast and robust earth mover's distances. In *2009 IEEE 12th international conference on computer vision*, 460–467. IEEE.
- Peyré, G.; Cuturi, M.; et al. 2019. Computational optimal transport: With applications to data science. *Foundations and Trends® in Machine Learning*, 11(5-6): 355–607.
- Pollard, D. 1982. Quantization and the method of k-means. *IEEE Transactions on Information theory*, 28(2): 199–205.
- Redko, I.; Courty, N.; Flamary, R.; and Tuia, D. 2019a. Optimal transport for multi-source domain adaptation under target shift. In *The 22nd AISTATS*, 849–858. PMLR.
- Redko, I.; Morvant, E.; Habrard, A.; Sebban, M.; and Bennani, Y. 2019b. *Advances in domain adaptation theory*. Elsevier.
- Reich, S. 2013. A nonparametric ensemble transform method for Bayesian inference. *SIAM Journal on Scientific Computing*, 35(4): A2013–A2024.
- Saenko, K.; Kulis, B.; Fritz, M.; and Darrell, T. 2010. Adapting visual category models to new domains. In *European conference on computer vision*, 213–226. Springer.
- Santambrogio, F. 2015. Optimal transport for applied mathematicians. *Birkhäuser, NY*, 55(58-63): 94.
- Schmitzer, B.; and Schnörr, C. 2013. A hierarchical approach to optimal transport. In *International Conference on Scale Space and Variational Methods in Computer Vision*, 452–464. Springer.
- Schölkopf, B.; Smola, A.; and Müller, K.-R. 1998. Nonlinear component analysis as a kernel eigenvalue problem. *Neural computation*, 10(5): 1299–1319.
- Shi, J.; and Malik, J. 2000. Normalized cuts and image segmentation. *IEEE Transactions on pattern analysis and machine intelligence*, 22(8): 888–905.
- Shimodaira, H. 2000. Improving predictive inference under covariate shift by weighting the log-likelihood function. *Journal of statistical planning and inference*, 90(2): 227–244.
- Stella, X. Y.; and Shi, J. 2003. Multiclass spectral clustering. In *Computer Vision, IEEE International Conference on*, volume 2, 313–313. IEEE Computer Society.
- Sugiyama, M.; Nakajima, S.; Kashima, H.; Von Buena, P.; and Kawanabe, M. 2007. Direct importance estimation with model selection and its application to covariate shift adaptation. In *NIPS*.
- Taherkhani, F.; Dabouei, A.; Soleymani, S.; Dawson, J.; and Nasrabadi, N. M. 2020. Transporting labels via hierarchical optimal transport for semi-supervised learning. In *ECCV*, 509–526.
- Vapnik, V. 2013. *The nature of statistical learning theory*. Springer science & business media.
- Villani, C. 2009. *Optimal transport: old and new*. Springer.

Wilson, G.; and Cook, D. J. 2020. A survey of unsupervised deep domain adaptation. *ACM Transactions on Intelligent Systems and Technology (TIST)*, 11(5): 1–46.

Yurochkin, M.; Clatici, S.; Chien, E.; Mirzazadeh, F.; and Solomon, J. M. 2019. Hierarchical Optimal Transport for Document Representation. In *Advances in Neural Information Processing Systems*.

Zha, H.; He, X.; Ding, C.; Gu, M.; and Simon, H. D. 2001. Spectral relaxation for k-means clustering. In *Advances in neural information processing systems*, 1057–1064.